scientific reports

Check for updates

OPEN

Structural and functional thalamic alterations in major depressive disorder with comorbid chronic pain

Jinzhong Ye, Caixia Xu, Huagui Guo, Wei Huang, Guojun Xie✉ & Jiaquan Liang✉

Major Depressive Disorder (MDD) is a prevalent mental health condition, often accompanied by chronic pain. This study investigates the structural and functional characteristics of the thalamus in individuals with MDD, both with and without comorbid pain, using magnetic resonance imaging (MRI) techniques. A total of 165 participants, including healthy controls, individuals with MDD, and those with comorbid depression and pain, were enrolled. The study found a reduction of the left thalamus in the MDD group, while no significant differences in thalamic volume were observed in the right thalamus or in the depression and pain comorbidity group. Functionally, no significant differences in fractional amplitude of low-frequency fluctuations (fALFF) and regional homogeneity (ReHo) were found between groups. However, correlation analysis revealed associations between thalamic structure and cognitive performance, as well as clinical symptom severity in the depression and pain comorbidity group. These findings highlight the thalamus's role in the pathophysiology of MDD and its interaction with chronic pain, suggesting potential targets for diagnostic and therapeutic strategies.

Keywords Major depressive disorder, Thalamus, Chronic pain, Neuroimaging, Fractional amplitude of low-frequency fluctuations (fALFF), Regional homogeneity (ReHo)

Major Depressive Disorder (MDD) is a widespread and incapacitating mental health condition that is characterized by persistent depressive symptoms, which substantially diminish an individual's functional capabilities and quality of life[1,2]. The prevalence of MDD is significant, with a considerable portion of patients experiencing comorbid chronic pain[3]. This comorbidity not only exacerbates the severity of the disorder but also poses a substantial challenge for clinical management and treatment outcomes[4].

Chronic pain is a prevalent condition that is often undertreated and can severely impact physical and psychological well-being[5]. When chronic pain co-occurs with MDD, it creates a complex clinical picture that is associated with greater symptom severity, increased functional impairment, and a higher burden on healthcare systems[6]. The pathophysiology of MDD with comorbid chronic pain is particularly intricate, as it involves an interaction between the neurobiological substrates of depression and the physiological processes of pain perception and regulation[7].

The thalamus, a central structure in the brain's neural networks, plays a pivotal role in sensory processing, cognitive function, and emotional regulation. It has been implicated in the pathogenesis of MDD[8], but its specific role in the context of comorbid chronic pain remains largely unexplored. Given the thalamus's integral involvement in both affective and sensory processing[9], it is hypothesized that this brain region may be significantly affected in individuals with MDD, particularly when compounded by chronic pain[10]. The complex interplay between mood disorders and chronic pain suggests that the thalamus might exhibit unique structural and functional characteristics in this subset of patients[11]. Specifically, coordinate-based meta-analyses have identified structural and functional thalamic alterations in individuals with MDD and chronic pain, underscoring the thalamus's dual role in affective and sensory processing[12–14]. These findings motivated our investigation into thalamic changes associated with MDD and chronic pain comorbidity.

Existing study has shown that MDD can lead to alterations in brain structure and function, with several studies reporting changes in thalamic volume and activity[15]. However, the majority of these studies have focused on MDD in the absence of comorbid pain, leaving a gap in our understanding of how chronic pain might modulate thalamic changes in depression. The fractional amplitude of low-frequency fluctuations (fALFF)

Department of Psychiatry, The Third People's Hospital of Foshan, Guangdong, People's Republic of China. ✉email: xiegjfs@126.com; liangjiaquan@muc.edu.cn

and regional homogeneity (ReHo) are promising metrics for assessing the functional integrity of the brain's resting-state networks, and their application in the study of MDD has provided valuable insights into the neural correlates of the disorder[16,17].

Given the complexity of MDD with comorbid chronic pain and the potential significance of the thalamus in its pathophysiology[18,19], the current study aims to investigate the structural and functional characteristics of the thalamus in individuals with MDD, both with and without comorbid chronic pain. By employing a comprehensive neuroimaging approach, including magnetic resonance imaging (MRI) techniques, we seek to elucidate the neural substrates underlying the interaction between MDD and chronic pain, with the hope of providing novel insights into the mechanisms that drive the exacerbation of symptoms and the potential for improved diagnostic and therapeutic strategies.

Method

Methodology

Subject recruitment

The enrollment of participants with MDD was conducted at the Third People's Hospital in Foshan, adhering to the diagnostic protocols outlined in the fifth edition of the Diagnostic and Statistical Manual of Mental Disorders (DSM-5). Chronic discomfort, defined as a persistent pain level of 3 or higher on a 0–10 numerical rating scale for the past week, and a duration exceeding three months, served as inclusion criteria[20]. Healthy controls (HC) were selected from the local community, meticulously matched with MDD participants in terms of age, gender, educational background, and other pertinent demographic variables. This study was approved by the ethics committee of the Third People's Hospital of Foshan (No. FSSY-LS202326), and the experiments were conducted following the declaration of Helsinki. Prior to participation, all patients and their legal guardians were comprehensively informed about the study's objectives and procedures, subsequently providing their written informed consent.

Inclusion and exclusion criteria

Participants were required to be of Han ethnicity, right-handed, experiencing a first episode of a drug-free mental disorder, and devoid of any familial history or comorbid conditions. The diagnosis of MDD was based on the DSM-5 criteria. Exclusion criteria encompassed contraindications to functional magnetic resonance imaging (fMRI), any brain pathology, a history of substance misuse, traumatic brain injuries, or neurologic disorders.

Assessment instruments

The assessment of participants involved the use of the Hamilton Depression Rating Scale (HAMD), Hamilton Anxiety Rating Scale (HAMA), and the Repeatable Battery for the Assessment of Neuropsychological Status (RBANS). The HAMD was utilized to quantify the severity of depressive symptoms. The HAMD was utilized to quantify the severity of depressive symptoms, with a cutoff score of ≥ 17 indicating moderate-to-severe depression[21]. Similarly, the HAMA was employed to assess anxiety severity, using a cutoff score of ≥ 14 to define clinically significant anxiety[22]. The RBANS was employed to evaluate cognitive functioning. This comprehensive neuropsychological assessment tool spans a broad range of cognitive domains including attention, memory, language, executive functions, and visual-spatial abilities, through a series of standardized tests and exercises. Designed for repetitive administration across multiple sessions, the RBANS facilitates the monitoring of cognitive performance over time, providing numerical scores that allow clinicians and researchers to compare an individual's cognitive abilities against standardized norms, accounting for variables such as age and education.

Magnetic resonance imaging protocols

Magnetic resonance imaging (MRI) scans, specifically structural T1-weighted images, were acquired using a General Electric 3 T Excite HD scanner, with the following parameters: repetition time (TR)/echo time (TE) = 8.6/3.3 milliseconds, flip angle (FA) = 9 degrees, field of view (FOV) = 240 mm × 240 mm, slice thickness = 4 mm, and a total of 172 slices. During these anatomical scans, participants were instructed to lie still inside the scanner, keep their eyes closed, and remain as motionless as possible to ensure high-quality image acquisition.

For the fMRI, the parameters were set to TR/TE = 2000/30 milliseconds, FA = 90 degrees, FOV = 240 mm × 240 mm, slice thickness = 4 mm, 36 slices, and a slice spacing of 1 mm. Participants were required to lie quietly with their eyes closed, relax, and avoid any intentional thought or movement, in order to capture the natural resting-state neural activity.

Analysis of low-frequency fluctuation amplitude

The fractional amplitude of low-frequency fluctuations (fALFF)[23] was analyzed using a methodologically validated approach. The power of each frequency within the low-frequency band ($0.01\ \text{Hz} < f < 0.1\ \text{Hz}$) was computed and divided by the total power across all frequencies to ascertain the fALFF value for each voxel. This value was further normalized by dividing it by the average signal amplitude of the entire brain to offset any variations in overall fALFF levels.

Volume-based morphometry (VBM) analysis

The VBM analysis was conducted using Statistical Parametric Mapping software version 8 (SPM8) following the standard procedures. The structural MRI scans were first segmented into gray matter, white matter, and cerebrospinal fluid. The gray matter segmentation was then normalized to the MNI-152 template, and the resulting images were modulated to correct for differences in brain size. The normalized and modulated gray matter images were smoothed with an 8 mm full-width at half-maximum (FWHM) Gaussian kernel to enhance

the signal-to-noise ratio[24]. The thalamic volumes were estimated by applying region-of-interest (ROI) analysis using the Wake Forest University (WFU) PickAtlas, which provides an automated method for ROI delineation. Estimation of Thalamic Volume: The volume of the left and right thalamus was estimated by applying the WFU PickAtlas to the normalized and smoothed gray matter images. The atlas contains predefined ROI masks for the thalamus, which were used to extract the volume of the left and right thalamus for each participant.

Investigation into regional homogeneity

The regional homogeneity (ReHo) analysis[25] entailed the aggregation of twenty-seven contiguous voxels and the utilization of Kendall's coefficient of concordance (KCC) to measure the similarity between a voxel and its twenty-six neighboring voxels. The standard brain template provided by the Data Processing Assistant for Resting-State fMRI (DPARSF) software was employed to generate KCC maps for each subject. Each voxel's KCC value was normalized by dividing it by the average KCC from the standard template, resulting in standardized ReHo maps.

Data preprocessing and analytical procedures

To ensure a comprehensive evaluation, all subjects were required to complete the scale assessments and fMRI data acquisition on the same day. Post-acquisition, fMRI datasets underwent visual inspection for quality control. During this process, 9 participants were excluded due to the presence of artifacts or noise that could compromise the integrity of the data. Subsequently, the fMRI images were normalized to the MNI-152 template using Statistical Parametric Mapping software version 8 (SPM8), and the functional data were registered to the corresponding structural MRI utilizing SPM8's registration tools. SPM8 was chosen for this process due to its well-established algorithms and widespread use in the field of neuroimaging. The normalization procedure included spatially warping the fMRI images to match the MNI-152 template, ensuring that the functional data could be compared across participants in a standardized space[24]. The functional data were then registered to the corresponding structural MRI utilizing SPM8's registration tools. This registration step was performed to align the functional data with the individual's structural scan, allowing for accurate localization of brain activity and structural features. To enhance the resolution and precision of the data, the fMRI datasets were resampled to a voxel size of 2 mm × 2 mm × 2 mm. The fMRI data were then smoothed with a Gaussian kernel having a FWHM of 8 mm to further refine the data quality.

The preprocessing pipeline for the fMRI data included the use of the Data Processing Assistant for Resting-State fMRI (DPARSF), SPM8, and cat12 software packages. This phase involved the quantification of thalamus volumes and the analysis of neural activity within regions using both fALFF and ReHo methodologies.

Data resampling and smoothing

To enhance the resolution and precision of the data, the fMRI datasets were resampled to a voxel size of 2 mm × 2 mm × 2 mm. This resampling process was performed to ensure consistency with the voxel size used in our structural data and standard atlases. The practice of upsampling has been employed in previous research to align voxel sizes across different types of neuroimaging data[26]. Following resampling, the fMRI data were smoothed with a Gaussian kernel having a FWHM of 8 mm to refine the data quality and enhance the signal-to-noise ratio. Subsequently, the ReHo maps were calculated based on the smoothed functional data.

Denoising and motion correction

The fMRI data underwent a rigorous denoising process to minimize noise and artifacts: Motion correction via regression of six motion parameters derived from realignment. Spike regression to remove transient spikes. Global Signal Regression (GSR), despite its controversial use, to regress out the global signal. Anatomical component-based correction (aCompCor) to remove non-neural noise related to respiratory and cardiac cycles. Framewise displacement (FD) was calculated, and participants with FD exceeding a predefined threshold were excluded to minimize motion artifacts. This preprocessing ensured optimal signal-to-noise ratio and reliable functional connectivity analysis.

The regions of interest (ROI) for this study were selected using the Wake Forest University (WFU) PickAtlas, an established neuroimaging tool that offers a library of anatomically defined ROI masks. The WFU PickAtlas was chosen for its reliability and ease of use in automated ROI delineation. The thalamic ROI was defined using the WFU PickAtlas mask for the thalamus, which is designed to capture the entire thalamic structure bilaterally. This mask was applied to the normalized and smoothed gray matter images to extract the thalamic volume for each participant.

Statistical analysis

The data were statistically processed using SPSS version 24.0. The Kolmogorov–Smirnov test was applied to ascertain the normal distribution of the data within each group. Confirming a normal distribution, one-way analysis of variance (ANOVA) was employed to determine statistical significance between groups, supplemented by post hoc testing. All results were reported as mean values ± standard deviation (SD). Pearson correlation analysis was conducted to explore the associations between thalamus volumes and functional metrics, as well as clinical data. To mitigate the risk of Type I errors due to multiple comparisons, p-values were corrected using appropriate statistical methods, ensuring the robustness and reliability of the findings. For Bayesian interpretation of null results, we applied *t*-tests and ANOVA-based Bayes factors (BF10) using the BayesFactor package in R (Morey and Rouder, 2018). Analyses focused on comparisons with nonsignificant classical p-values ($p > 0.05$). Default settings were used (Cauchy prior width = 0.707 for *t*-tests; scaled t-distribution prior for ANOVA). BF10 < 1 indicated evidence for the null hypothesis, and values were interpreted following Jefferies' scale: 3–10 = moderate evidence, > 10 = strong evidence.

VBM and functional amplitude (fALFF/ReHo) analyses were conducted in SPM 8. Data were normalized to MNI space, smoothed, and adjusted for age, sex, and intracranial volume (VBM) or framewise displacement (fALFF/ReHo). False Discovery Rate (FDR) correction (voxel-level $p < 0.05$) was prioritized; uncorrected results are reported for completeness. Voxel-wise Bayesian Parameter Maps (BPM) were calculated within the SPM8 software framework, which natively supports Bayesian inference for neuroimaging data. Specifically, the analysis utilized SPM8's implementation of Bayesian parameter estimation, incorporating default Cauchy priors (scale = 0.707) as specified in the Methods section. This approach allowed them to estimate Bayes Factors (BF_{10}) for voxels across the brain.

Results

Demographic profile of participants

A total of 165 individuals were enrolled in this study, comprising HC ($n = 46$), individuals with MDD ($n = 38$), and those with comorbid depression and pain ($n = 32$). The HC, MDD, and depression and pain comorbidity groups exhibited no significant differences in age, gender, and educational attainment (Table 1). Moreover, the depression and pain comorbidity group demonstrated elevated HAMD and HAMA scores compared to the MDD group. No significant disparities in RBANS scores were observed among the HC, MDD, and depression and pain comorbidity groups (Table 1).

Thalamus insights

With respect to brain volume, the MDD group exhibited significant left thalamic volume reduction compared to HCs ($p < 0.01$). However, no significant variations were detected in the volume of the right thalamus across the HC, MDD, and depression and pain comorbidity groups. In terms of functional metrics, no significant differences in fALFF and ReHo were found among the HC, MDD, and depression and pain comorbidity groups (Table 2; Fig. 1). BF10 < 1 across all group comparisons for the right thalamus (MDD vs. HC: BF10 = 0.42) and DPC left thalamus (BF10 = 0.15), indicating moderate-to-strong evidence against volumetric differences in these regions (Supplemental Table 1). No evidence for group differences in fALFF (right thalamus: BF10 = 0.28) or ReHo (left thalamus: BF10 = 0.12), consistent with null results from classical tests (Supplemental Table 2).

Correlation analysis utilizing Pearson's method

Pearson's correlation analysis revealed several significant correlations within the depression and pain comorbidity group (Table 3). Notably, fALFF and ReHo values in the right thalamus were inversely correlated with HAMD scores (fALFF: $r = -0.44$, $p = 0.02$; ReHo: $r = -0.37$, $p = 0.049$) and HAMA scores (fALFF: $r = -0.38$, $p = 0.04$; ReHo: $r = -0.44$, $p = 0.02$). Additionally, the volume of the left and right thalamus was positively

	HC	MDD	Depression and pain comorbidity	F	*P*-value
Participants	46	38	32		
Age (years)	35.83 ± 13.16	30.16 ± 13.55	31.47 ± 12.72	2.19	0.12
Gender (M/F)	19/27	14/24	11/21	0.2	0.82
Education				0.2	0.82
Below 9 years, n (%)	14 (30%)	10 (26%)	8 (25%)		
10–12 years, n (%)	6 (13%)	10 (26%)	5 (16%)		
13–17 years, n (%)	26 (57%)	18 (48%)	19 (59%)		
mBPI			4.38 ± 1.62		
HAMD score	2.5 ± 3.67	21.00 ± 7.02**	25.76 ± 6.95**##	179.7	< 0.0001
HAMA score	2.02 ± 2.58	13.00 ± 4.44**	19.41 ± 4.86**##	192.7	< 0.0001
RBANS					
Immediate memory (learning)	27.63 ± 7.03	26.70 ± 6.66	25.53 ± 6.28	0.88	0.42
Immediate memory (story memory)	14.41 ± 5.96	12.63 ± 5.36	13.03 ± 5.83	0.98	0.38
Visuospatial construction	17.76 ± 2.41	18.59 ± 2.45	18.30 ± 2.37	1.11	0.33
Language	18.28 ± 4.34	16.59 ± 4.43	18.33 ± 4.84	1.43	0.24
Attention (digit span)	14.13 ± 2.18	13.48 ± 2.93	13.53 ± 2.54	0.79	0.46
Attention (coding)	49.80 ± 14.15	44.70 ± 14.69	47.70 ± 11.64	1.2	0.31
Delayed memory (list recall)	6.61 ± 3.11	5.89 ± 3.04	5.80 ± 2.92	0.82	0.44
Delayed memory (list recognition)	19.54 ± 1.05	19.33 ± 1.30	19.40 ± 1.10	0.33	0.72
Delayed memory (story recall)	7.52 ± 3.74	6.44 ± 3.91	7.57 ± 3.44	0.87	0.42
Delayed memory (figure recall)	14.46 ± 4.71	13.56 ± 4.40	13.47 ± 4.09	0.58	0.56

Table 1. Description of clinical scales among healthy control, major depressive disorder, and depression and pain comorbidity. *HC* healthy control, *MDD* major depressive disorder, *HAMD* Hamilton Depression Scale, *HAMA* Hamilton Anxiety Scale, *mBPI* Modified Brief Pain Inventory, *RBANS* Repeatable Battery for the Assessment of Neuropsychological Status; **$p < 0.01$ compared to HC group; ##$p < 0.01$ compared to MDD group.

	HC	MDD	Depression and pain comorbidity	F	*P*-value
Volume (cm^3)					
Thalamus (left)	3.60 ± 0.55	3.24 ± 0.35**	3.50 ± 0.49	5.82	0.0036
Thalamus (right)	3.35 ± 0.48	3.37 ± 0.43	3.56 ± 0.60	1.9	0.16
FALFF					
Thalamus (left)	− 0.42 ± 0.23	− 0.36 ± 0.20	− 0.47 ± 0.30	1.7	0.19
Thalamus (right)	− 0.42 ± 0.22	− 0.355 ± 0.23	− 0.40 ± 0.28	0.88	0.42
ReHo					
Thalamus (left)	− 0.27 ± 0.27	− 0.25 ± 0.20	− 0.34 ± 0.28	1.21	0.3
Thalamus (right)	− 0.30 ± 0.24	− 0.23 ± 0.23	− 0.26 ± 0.28	0.85	0.43

Table 2. Comparison of MRI data among healthy control, major depressive disorder, and depression and pain comorbidity. *HC* healthy control, *MDD* major depressive disorder, *FALFF* fractional amplitude of low frequency fluctuation, *ReHo* regional homogeneity; The fALFF and ReHo values were measured in normalized unit arbitrary unit. $^{**}p < 0.01$ compared to HC group.

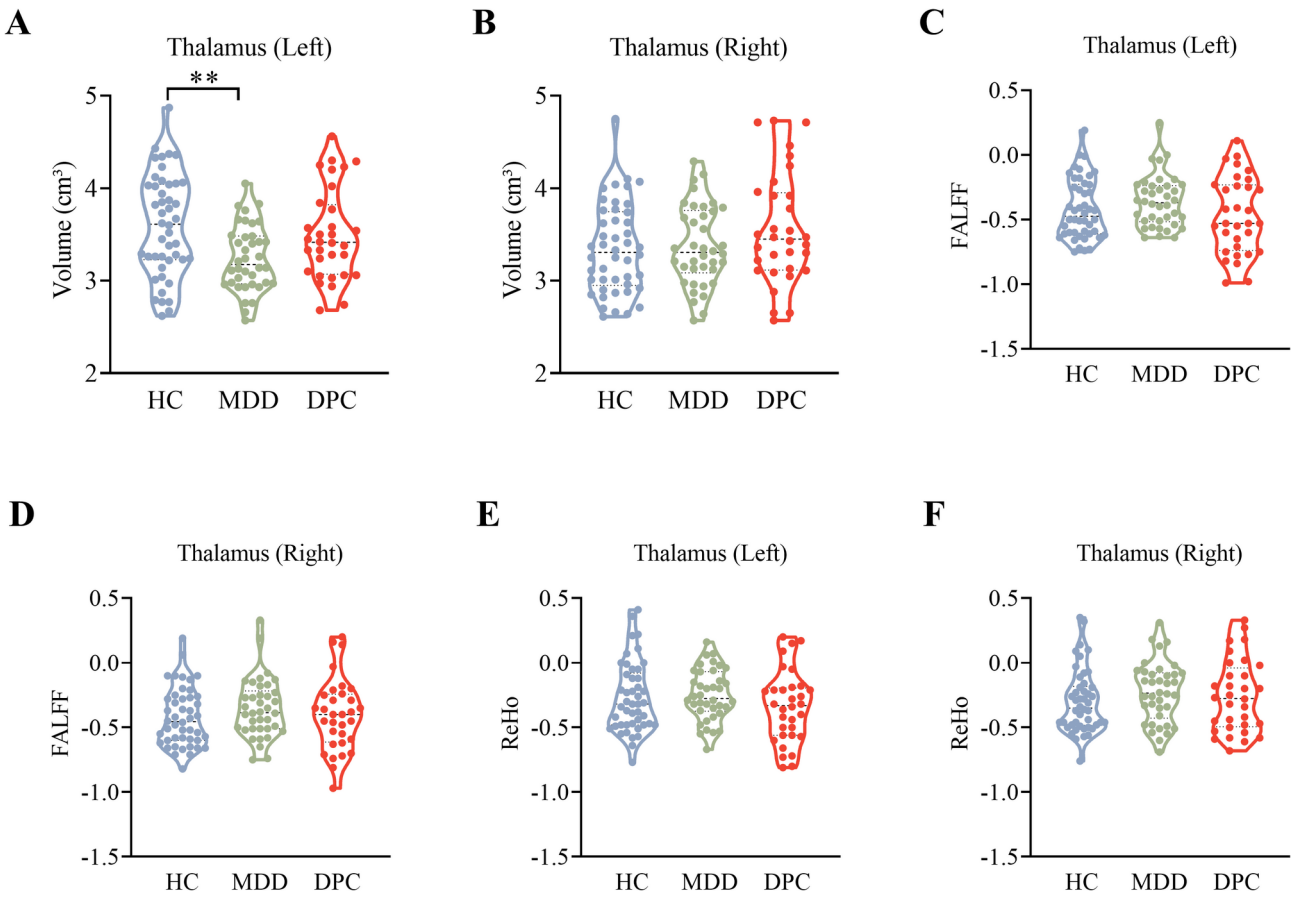

Fig. 1. The violin plots of healthy control, major depressive disorder, and depression and pain comorbidity. *HC* healthy control, *MDD* major depressive disorder, *DPC* Depression and pain comorbidity, *FALFF* fractional amplitude of low frequency fluctuation, *ReHo* regional homogeneity; The fALFF and ReHo values were measured in normalized unit arbitrary unit. $^{**}p < 0.01$ compared to HC group.

correlated with immediate memory (Story Memory) (left: $r = 0.45$, $p = 0.02$; right: $r = 0.47$, $p = 0.008$), delayed memory (List Recall) (left: $r = 0.45$, $p = 0.01$; right: $r = 0.48$, $p = 0.008$), delayed memory (List Recognition) (left: $r = 0.49$, $p = 0.006$; right: $r = 0.46$, $p = 0.01$), and delayed memory (Story Recall) (left: $r = 0.48$, $p = 0.007$; right: $r = 0.56$, $p = 0.001$). Furthermore, the volume of the right thalamus was positively correlated with visuospatial construction abilities ($r = 0.43$, $p = 0.02$). The inverse relationship between DPC patients' HAMA scores and right thalamic ReHo ($r = -0.44$, $p = 0.049$) gained weak Bayesian support (BF10 = 2.1). In contrast, significant positive correlations (e.g., left thalamic volume with memory performance) were reinforced by moderate evidence (BF10 = 3.8) (Supplemental Table 3).

		Volume		FALFF		ReHo	
		Thalamus (left)	Thalamus (right)	Thalamus (left)	Thalamus (right)	Thalamus (left)	Thalamus (right)
HAMD	r	0.009	0.03	−0.24	−0.44	−0.23	−0.37
	P	0.96	0.86	0.21	**0.02***	0.23	**0.049***
HAMA	r	−0.14	−0.1	−0.37	−0.38	−0.3	−0.44
	P	0.47	0.61	0.05	**0.04***	0.12	**0.02***
Immediate memory (learning)	r	0.19	0.19	0.07	0.07	0.16	0.19
	P	0.31	0.32	0.7	0.71	0.41	0.32
Immediate memory (story memory)	r	0.45	0.47	0.11	0.12	0.16	0.18
	P	**0.02***	**0.008****	0.56	**0.52**	0.39	0.35
Visuospatial construction	r	0.34	0.43	0.17	0.12	0.26	0.19
	P	0.06	**0.02***	0.37	0.52	0.16	0.31
Language	r	−0.008	0.03	−0.07	0.08	0.03	0.16
	P	0.96	0.89	0.69	0.67	0.88	0.41
Attention (digit span)	r	0.08	0.07	−0.13	−0.03	−0.03	0.03
	P	0.66	0.71	0.5	0.86	0.86	0.85
Attention (coding)	r	0.3	0.31	0.45	−0.03	0.05	0.04
	P	0.11	0.1	0.81	0.88	0.79	0.85
Delayed memory (list recall)	r	0.45	0.48	0.007	0.04	0.05	0.16
	P	**0.01***	**0.008****	0.97	0.84	0.79	0.41
Delayed memory (list recognition)	r	0.49	0.46	0.1	0.11	0.04	0.06
	P	**0.006****	**0.01***	0.61	0.55	0.84	0.74
Delayed memory (story recall)	r	0.48	0.56	0.22	0.11	0.29	0.2
	P	**0.007****	**0.001****	0.25	0.54	0.12	0.28
Delayed memory (figure recall)	r	0.09	0.14	-0.14	-0.07	0.008	0.00001
	P	0.62	0.46	0.45	0.71	0.97	0.99

Table 3. Correlation coefficients between behavioral measures and brain metrics with FDR correction for multiple comparisons. *HAMD* Hamilton Depression Scale, *HAMA* Hamilton Anxiety Scale, *FALFF* fractional amplitude of low frequency fluctuation, *ReHo* regional homogeneity. Significant values are in bold.

Significant correlations reflect findings that survived FDR correction. For example, the inverse correlation between Right Thalamus ReHo and HAMA ($r = -0.44$) has an uncorrected p-value of 0.01, but FDR correction raises it to 0.02, still remaining significant ($q < 0.05$). In contrast, the correlation between Left Thalamus Volume and Visuospatial Construction has an uncorrected $p = 0.04$, but the FDR-corrected $p = 0.06$, thus becoming nonsignificant (Supplemental Table 4).

Exploratory voxel-wise subgroup analyses

To explore spatially distributed patterns beyond our ROI analysis, exploratory voxel-wise subgroup comparisons were performed using classical FDR correction ($p < 0.05$) and BPM (BF10 > 3). In the VBM analysis, MDD patients showed marginally significant gray matter reduction in the left thalamus (peak coordinates: x = −12, y = −18, z = 6; t = 4.13; FDR $p = 0.057$) and right ACC (x = 4, y = 30, z = 24; t = 3.89; FDR $p = 0.075$). Bayesian analysis provided moderate evidence for thalamic atrophy (BF10 = 4.2) in MDD. Pain-depression comorbidity cases did not show significant structural differences compared to HCs. Functional analyses revealed reduced left DLPFC fALFF in MDD (BF10 = 2.4) and right insula hyperactivation in comorbid patients (t = 3.32, $p = 0.001$ uncorrected) (Supplemental Table 5). These results, while preliminary, align with our ROI findings and warrant further investigation in larger cohorts.

Discussion

Our findings provide several key insights into the neural substrates of MDD, particularly in relation to thalamic structure and function, and its interaction with chronic pain. The study enrolled a total of 165 participants, including HC, individuals with MDD, and those with comorbid depression and pain, which allowed for a comprehensive examination of the thalamic changes associated with these conditions.

The structural MRI analysis revealed a reduction of the left thalamus in MDD patients compared to HC, consistent with prior studies demonstrating locus-specific thalamic volumetric changes in depression[27]. The asymmetric left thalamic vulnerability may arise from its specialized role in integrating emotional and cognitive processes through connectivity with prefrontal and limbic networks[28]. Notably, thalamic atrophy in depression has been linked to clinical severity in other research[29], suggesting its involvement in symptom expression. The absence of significant volume differences in the right thalamus or comorbidity group highlights the nuanced anatomical specificity of these changes. Notably, no significant differences in thalamic volume were observed in the right thalamus or in the depression and pain comorbidity group. The lack of statistical significance may

be due to either the actual absence of differences or low statistical power, rather than directly highlighting the complexity of the neuroanatomical changes in MDD.

Functionally, our results did not show significant differences in fALFF and ReHo among the HC, MDD, and depression and pain comorbidity groups. However, the absence of significant differences does not necessarily imply that the functional connectivity and activity within the thalamus remain relatively preserved. There could be other factors contributing to this lack of significance. However, the lack of significant functional differences could also be influenced by the inherent variability in resting-state fMRI data, the sample size, or the specific methodologies employed. It is possible that more subtle or regionally specific changes in thalamic function were not captured by our analysis. Future studies with larger sample sizes, more sensitive analysis techniques, or specific task-based fMRI paradigms may be able to detect more nuanced functional alterations.

The correlation analysis revealed intriguing associations between thalamic structure and cognitive performance, as well as clinical symptom severity in the depression and pain comorbidity group[30]. Specifically, we found that fALFF and ReHo values in the right thalamus were inversely correlated with HAMD and HAMA scores. This suggests that thalamic functional integrity may be related to the severity of depressive and anxiety symptoms in individuals with comorbid depression and pain[31]. Furthermore, the positive correlations between thalamic volume and various memory and visuospatial construction abilities highlight the thalamus's role in cognitive functioning, which may be compromised in MDD, particularly when accompanied by chronic pain. The inclusion of Bayesian statistics addresses recent methodological calls for rigor in interpreting nonsignificant results[32,33]. The support for null hypotheses in structural volume comparisons (right thalamus differences) suggests that MDD and chronic pain comorbidity might involve nonspecific mechanisms (compensatory proliferation) for right thalamic regions. Strong null evidence for functional metrics (fALFF/ReHo) indicates that resting-state functional alterations may be more pronounced in non-thalamic regions or task-based paradigms. Weak support for marginal correlations (HAMA and ReHo) highlights the need for larger samples to validate directionalities. These Bayesian results complement classical statistical findings, jointly emphasizing the thalamus' subregion-specific role in depression-pain interactions.

These findings have important implications for the understanding and treatment of MDD, especially in cases with comorbid pain. The thalamus, as a central hub for sensory processing and integration, may play a critical role in the pathophysiology of both MDD and chronic pain[34,35]. Our results suggest that targeting the thalamus could be a viable strategy for the development of novel therapeutic interventions for MDD, particularly in patients with comorbid pain. Therapies that aim to modulate thalamic activity, such as transcranial magnetic stimulation (TMS) or deep brain stimulation (DBS)[36], could potentially alleviate both depressive symptoms and pain, offering a more holistic approach to treatment[37]. The inverse correlations between thalamic fALFF and ReHo values and clinical symptom severity scores further suggest that thalamic functional integrity could serve as a biomarker for disease progression and treatment response. Monitoring changes in thalamic function over the course of treatment could provide valuable insights into the efficacy of various therapeutic interventions[38,39]. These findings highlight the potential role of subcortical-cortical dysconnectivity (e.g., thalamus-ACC interactions) in MDD and thalamic-insula hyperactivation in comorbidity cases. While further validation is required, these data form the basis for ongoing studies using longitudinal and multivariate analysis.

However, it is important acknowledge the limitations of this study. The cross-sectional design does not allow for the determination of causality, and the findings should be interpreted with caution. Longitudinal studies are needed to track the changes in thalamic structure and function over time and in relation to the course of the disorder and treatment. Additionally, while we have controlled for several demographic variables, there may be other confounding factors that could influence the results, such as medication status or lifestyle factors. This study contributes to the growing body of research on the neural substrates of MDD, particularly focusing on the role of the thalamus in both MDD and its comorbidity with chronic pain. The findings suggest that the thalamus may undergo structural changes in MDD, particularly in the left thalamus, and that its functional integrity is associated with the severity of clinical symptoms and cognitive performance in individuals with comorbid depression and pain.

In summary, the present study adds to the literature by providing evidence of thalamic involvement in MDD, particularly in the context of comorbid pain. The structural and functional insights gained from this research contribute to a deeper understanding of the neural bases of MDD and suggest new directions for both research and clinical practice. As we continue to unravel the complexities of MDD, the thalamus stands out as a promising area of focus for the development of novel treatments and biomarkers, with the potential to significantly enhance the lives of those affected by this disabling condition.

Author contributions

JQ L and GJ X designed the study; JZ Y, CX X and HG G collected the data; JZ Y and W H performed the analysis. JZ Y and CX X drafted the manuscript with critical revisions from all authors.

Data availability

All relevant data are within the manuscript and its Additional files. The data are available from the corresponding author on reasonable request.

Received: 18 September 2024; Accepted: 28 April 2025
Published online: 15 May 2025

References

1. Cui, L. et al. Major depressive disorder: Hypothesis, mechanism, prevention and treatment. *Signal. Transduct. Target. Ther.* **9**. https://doi.org/10.1038/s41392-024-01738-y (2024).
2. Gray, J. P., Müller, V. I., Eickhoff, S. B. & Fox, P. T. Multimodal abnormalities of brain structure and function in major depressive disorder: A meta-analysis of neuroimaging studies. *Am. J. Psychiatry* **177**, 422–434. https://doi.org/10.1176/appi.ajp.2019.19050560 (2020).
3. Bair, M. J., Robinson, R. L., Katon, W. & Kroenke, K. Depression and pain comorbidity: A literature review. *Arch. Intern. Med.* **163**, 2433–2445. https://doi.org/10.1001/archinte.163.20.2433 (2003).
4. Corlier, J. et al. Repetitive transcranial magnetic stimulation treatment of major depressive disorder and comorbid chronic pain: Response rates and neurophysiologic biomarkers. *Psychol. Med.* **53**, 823–832. https://doi.org/10.1017/s0033291721002178 (2023).
5. Cohen, S. P., Vase, L. & Hooten, W. M. Chronic pain: An update on burden, best practices, and new advances. *Lancet (London England)* **397**, 2082–2097. https://doi.org/10.1016/s0140-6736(21)00393-7 (2021).
6. Jolly, T. et al. Risk of suicide in patients with major depressive disorder and comorbid chronic pain disorder: An insight from national inpatient sample data. *Pain Physician*. **25**, 419–425 (2022).
7. Jaracz, J., Gattner, K., Jaracz, K. & Górna, K. Unexplained painful physical symptoms in patients with major depressive disorder: Prevalence, pathophysiology and management. *CNS Drugs* **30**, 293–304. https://doi.org/10.1007/s40263-016-0328-5 (2016).
8. Zhang, F. F., Peng, W., Sweeney, J. A., Jia, Z. Y. & Gong, Q. Y. Brain structure alterations in depression: Psychoradiological evidence. *CNS Neurosci. Ther.* **24**, 994–1003. https://doi.org/10.1111/cns.12835 (2018).
9. Gao, C., Weber, C. E. & Shinkareva, S. V. The brain basis of audiovisual affective processing: Evidence from a coordinate-based activation likelihood estimation meta-analysis. *Cortex* **120**, 66–77. https://doi.org/10.1016/j.cortex.2019.05.016 (2019).
10. Lee, M. J. et al. Effects of acupuncture on chronic stress-induced depression-like behavior and its central neural mechanism. *Front. Psychol.* **10**, 1353. https://doi.org/10.3389/fpsyg.2019.01353 (2019).
11. Farb, N. A., Anderson, A. K. & Segal, Z. V. The mindful brain and emotion regulation in mood disorders. *Can. J. Psychiatry*. **57**, 70–77. https://doi.org/10.1177/070674371205700203 (2012).
12. Li, J., Kuang, S., Liu, Y., Wu, Y. & Li, H. Structural and functional brain alterations in subthreshold depression: A multimodal coordinate-based meta-analysis. *Hum. Brain Mapp.* **45**, e26702. https://doi.org/10.1002/hbm.26702 (2024).
13. Diener, C. et al. A meta-analysis of neurofunctional imaging studies of emotion and cognition in major depression. *NeuroImage* **61**, 677–685. https://doi.org/10.1016/j.neuroimage.2012.04.005 (2012).
14. Friebel, U., Eickhoff, S. B. & Lotze, M. Coordinate-based meta-analysis of experimentally induced and chronic persistent neuropathic pain. *NeuroImage* **58**, 1070–1080. https://doi.org/10.1016/j.neuroimage.2011.07.022 (2011).
15. Han, K. M., De Berardis, D., Fornaro, M. & Kim, Y. K. Differentiating between bipolar and unipolar depression in functional and structural MRI studies. *Prog Neuro-psychopharmacol Biol. Psychiatry*. **91**, 20–27. https://doi.org/10.1016/j.pnpbp.2018.03.022 (2019).
16. Zhou, Y. et al. A resting state functional magnetic resonance imaging study of unmedicated adolescents with non-suicidal self-injury behaviors: Evidence from the amplitude of low-frequency fluctuation and regional homogeneity indicator. *Front. Psychiatry*. **13**, 925672. https://doi.org/10.3389/fpsyt.2022.925672 (2022).
17. Li, G. Z., Liu, P. H., Zhang, A. X., Andari, E. & Zhang, K. R. A resting state fMRI study of major depressive disorder with and without anxiety. *Psychiatry Res.* **315**, 114697. https://doi.org/10.1016/j.psychres.2022.114697 (2022).
18. Drago, T. et al. A comprehensive regional neurochemical theory in depression: A protocol for the systematic review and meta-analysis of 1H-MRS studies in major depressive disorder. *Syst. Rev.* **7**, 158. https://doi.org/10.1186/s13643-018-0830-6 (2018).
19. Nascimento, S. S., Oliveira, L. R. & DeSantana, J. M. Correlations between brain changes and pain management after cognitive and meditative therapies: A systematic review of neuroimaging studies. *Complement. Ther. Med.* **39**, 137–145. https://doi.org/10.1016/j.ctim.2018.06.006 (2018).
20. Knowles, L. M. et al. Early treatment improvements in depression are associated with overall improvements in fatigue impact and pain interference in adults with multiple sclerosis. *Ann. Behav. Med.* **55**, 833–843. https://doi.org/10.1093/abm/kaaa102 (2021).
21. Rosenberg, L. I. The Ham-D is not Hamilton's depression scale. *Psychopharmacol. Bull.* **52**, 117–153 (2022).
22. Tung, V. S. et al. Diagnostic value in screening severe depression of the Hamilton depression rating scale, Hamilton anxiety rating scale, Beck depression inventory scale, and Zung's Self-Rating anxiety scale among patients with recurrent depression disorder. *Acta Inf. Med.* **31**, 249–253. https://doi.org/10.5455/aim.2023.31.249-253 (2023).
23. Chen, W. et al. Differences in fractional amplitude of low-frequency fluctuations (fALFF) and cognitive function between untreated major depressive disorder and schizophrenia with depressive mood patients. *BMC Psychiatry* **24**, 313. https://doi.org/10.1186/s12888-024-05777-1 (2024).
24. Huang, S. et al. Distinguishing functional and structural MRI abnormalities between bipolar and unipolar depression. *Front. Psychiatry* **14**, 1343195. https://doi.org/10.3389/fpsyt.2023.1343195 (2023).
25. Geng, J. et al. Altered regional homogeneity in patients with somatic depression: A resting-state fMRI study. *J. Affect. Disord.* **246**, 498–505. https://doi.org/10.1016/j.jad.2018.12.066 (2019).
26. Birn, R. M. Quality control procedures and metrics for resting-state functional MRI. *Front. Neuroimaging.* **2**, 1072927. https://doi.org/10.3389/fnimg.2023.1072927 (2023).
27. Lu, Y. et al. The volumetric and shape changes of the putamen and thalamus in first episode, untreated major depressive disorder. *NeuroImage Clin.* **11**, 658–666. https://doi.org/10.1016/j.nicl.2016.04.008 (2016).
28. Yun, J. Y., Choi, S. H., Park, S. & Jang, J. H. Association of executive function with suicidality based on resting-state functional connectivity in young adults with subthreshold depression. *Sci. Rep.* **13**, 20690. https://doi.org/10.1038/s41598-023-48160-y (2023).
29. Yang, H. G. et al. Altered voxel-level whole-brain functional connectivity in multiple system atrophy patients with depression symptoms. *BMC Psychiatry* **22**, 279. https://doi.org/10.1186/s12888-022-03893-4 (2022).
30. Roy, D. S., Zhang, Y., Halassa, M. M. & Feng, G. Thalamic subnetworks as units of function. *Nat. Neurosci.* **25**, 140–153. https://doi.org/10.1038/s41593-021-00996-1 (2022).
31. Shang, B. et al. Higher blood-brain barrier permeability in patients with major depressive disorder identified by DCE-MRI imaging. *Psychiatry Res. Neuroimaging* **337**, 111761. https://doi.org/10.1016/j.pscychresns.2023.111761 (2024).
32. Dienes, Z. Using Bayes to get the most out of non-significant results. *Front. Psychol.* **5**, 781. https://doi.org/10.3389/fpsyg.2014.00781 (2014).
33. Keysers, C., Gazzola, V. & Wagenmakers, E. J. Using Bayes factor hypothesis testing in neuroscience to establish evidence of absence. *Nat. Neurosci.* **23**, 788–799. https://doi.org/10.1038/s41593-020-0660-4 (2020).
34. Hao, Z. et al. Pain avoidance and functional connectivity between Insula and amygdala identifies suicidal attempters in patients with major depressive disorder using machine learning. *Psychophysiology* **60**, e14136. https://doi.org/10.1111/psyp.14136 (2023).
35. Nugent, A. C. et al. Multimodal imaging reveals a complex pattern of dysfunction in corticolimbic pathways in major depressive disorder. *Hum. Brain Mapp.* **40**, 3940–3950. https://doi.org/10.1002/hbm.24679 (2019).
36. Wang, Z. et al. Increased thalamic gray matter volume induced by repetitive transcranial magnetic stimulation treatment in patients with major depressive disorder. *Front. Psychiatry* **14**, 1163067. https://doi.org/10.3389/fpsyt.2023.1163067 (2023).
37. Cash, R. F. H. et al. A multivariate neuroimaging biomarker of individual outcome to transcranial magnetic stimulation in depression. *Hum. Brain Mapp.* **40**, 4618–4629. https://doi.org/10.1002/hbm.24725 (2019).

38. Hamon, M. & Blier, P. Monoamine neurocircuitry in depression and strategies for new treatments. *Prog Neuro-psychopharmacol. Biol. Psychiatry* **45**, 54–63. https://doi.org/10.1016/j.pnpbp.2013.04.009 (2013).
39. Huang, F. F. et al. Predicting responses to cognitive behavioral therapy in obsessive-compulsive disorder based on multilevel indices of rs-fMRI. *J. Affect. Disord.* **323**, 345–353. https://doi.org/10.1016/j.jad.2022.11.073 (2023).

Author contributions

JQ L and GJ X designed the study; JZ Y, CX X and HG G collected the data; JZ Y and W H performed the analysis. JZ Y and CX X drafted the manuscript with critical revisions from all authors.

Funding

The Medical Science and Technology Research Fund Project of Guangdong Province(A2024206), the project of Foshan Science and Technology Bureau (2320001006089, 2220001004473), and the Foshan "14th five-year plan" medical high level key psychiatric specialty construction project (FSGSP145069).

Declarations

Competing interests

The authors declare no competing interests.

Additional information

Supplementary Information The online version contains supplementary material available at https://doi.org/10.1038/s41598-025-00431-6.

Correspondence and requests for materials should be addressed to G.X. or J.L.

Reprints and permissions information is available at www.nature.com/reprints.

Publisher's note Springer Nature remains neutral with regard to jurisdictional claims in published maps and institutional affiliations.